



Unified correlation between SPT–N and shear wave velocity for a wide range of soil types considering strain-dependent behavior

Chi-Chin Tsai^{a,*}, Tadahiro Kishida^b, Chun-Hsiang Kuo^c

^a Department of Civil Engineering, National Chung Hsing University, Taiwan

^b Civil Infrastructure and Environmental Engineering, Khalifa University of Science Technology & Research, United Arab Emirates

^c National Center for Research on Earthquake Engineering, Taiwan

ABSTRACT

The shear wave velocity (V_s) of sediments plays a key role in seismic wave amplification and is required in site response analysis. Such information is usually lacking during field exploration, but standard penetration test blow count (N) is typically available. Therefore, several studies have established empirical correlations between N and V_s for engineering use. However, these empirical correlations significantly vary in terms of model form and are only applicable to specific soil types, such as sand or clay. A unified empirical correlation for a wide range of soil types, which contains several soil properties (e.g., liquid limit and plasticity index (PI)) in addition to the V_s and N of strata, is developed in this study using the Engineering Geological Database for the Taiwan Strong Motion Instrumentation Program. Influences of confining stress, fines content (FC), PI, and soil types on small-strain properties (i.e., V_s) and large-strain measurements (i.e., N) are first evaluated through the developed correlations with these parameters. The unified correlation between V_s and N that is dependent on confining stress, FC, and PI is then proposed through the conditional prediction approach. The model successfully applies to different regions in Taiwan that includes various types of soil deposits and, thus, is potentially used for the other regions.

1. Introduction

A key property required to effectively estimate the seismic response of a site is small-strain shear modulus G_o , which is often computed by measuring shear wave velocity (V_s) and mass density (ρ) as follows:

$$G_o = \rho V_s^2. \quad (1)$$

The importance of G_o has been widely recognized in site response analysis and ground motion prediction. The site response analysis requires V_s profile as input parameters [1], while the advanced ground motion prediction equations implement site factors based on V_s of upper 30 m [2,3]. Geophysical investigations are typically performed to measure the V_s profile. However, these measurements are not always common due to the additional cost of field investigation. Therefore, correlations between V_s and standard penetration test (SPT) blow count (N), which is conditioned on the geologic setting and soil types, are potentially useful for the aforementioned situation.

Numerous relations between N and V_s have been established in previous research [4–11]. However, these empirical correlations developed mainly by statistical method significantly vary in terms of model form and are limited to a specific soil type (e.g., sand or clay) or a specific site/region [12]. The development of these correlations also lacks theoretical or experimental support. Therefore, this study aims to establish a unified correlation between N and V_s that can be applied to a

wide range of soil types with an experimental and statistical basis. The Engineering Geological Database (EGDT) for the Taiwan Strong Motion Instrumentation Program (TSMIP) [11] is utilized in the analysis. Factors that can change the small-strain properties of G_o are reviewed based on the collected literature. Based on the previous study on laboratory test data, a model form that describes the small-strain properties (i.e., V_s) and the large-strain measurements (i.e., N) is proposed. The influence of effective overburden stress (σ'_v), fines content (FC), plasticity index (PI), and overconsolidation ratio (OCR) on small-strain properties and large-strain measurements is evaluated according to the regression analysis results. A unified correlation between V_s and N that is dependent on these parameters is then proposed through the conditional prediction approach.

2. Correlation form of v_s and N

2.1. Fundamental functional form of G_o

The most common functional form of the relations of G_o as proposed in the literature [13] is as follows:

$$G_o = A \cdot F(e)(\sigma'_0)^n \quad (2)$$

where σ'_0 is effective confining stress, $F(e)$ is the function of void ratio, and constants A and n are determined by statistical regression of

* Corresponding author.

E-mail addresses: tsaicc@nchu.edu.tw (C.-C. Tsai), kishidapple@gmail.com (T. Kishida), chkuo@ncree.narl.org.tw (C.-H. Kuo).

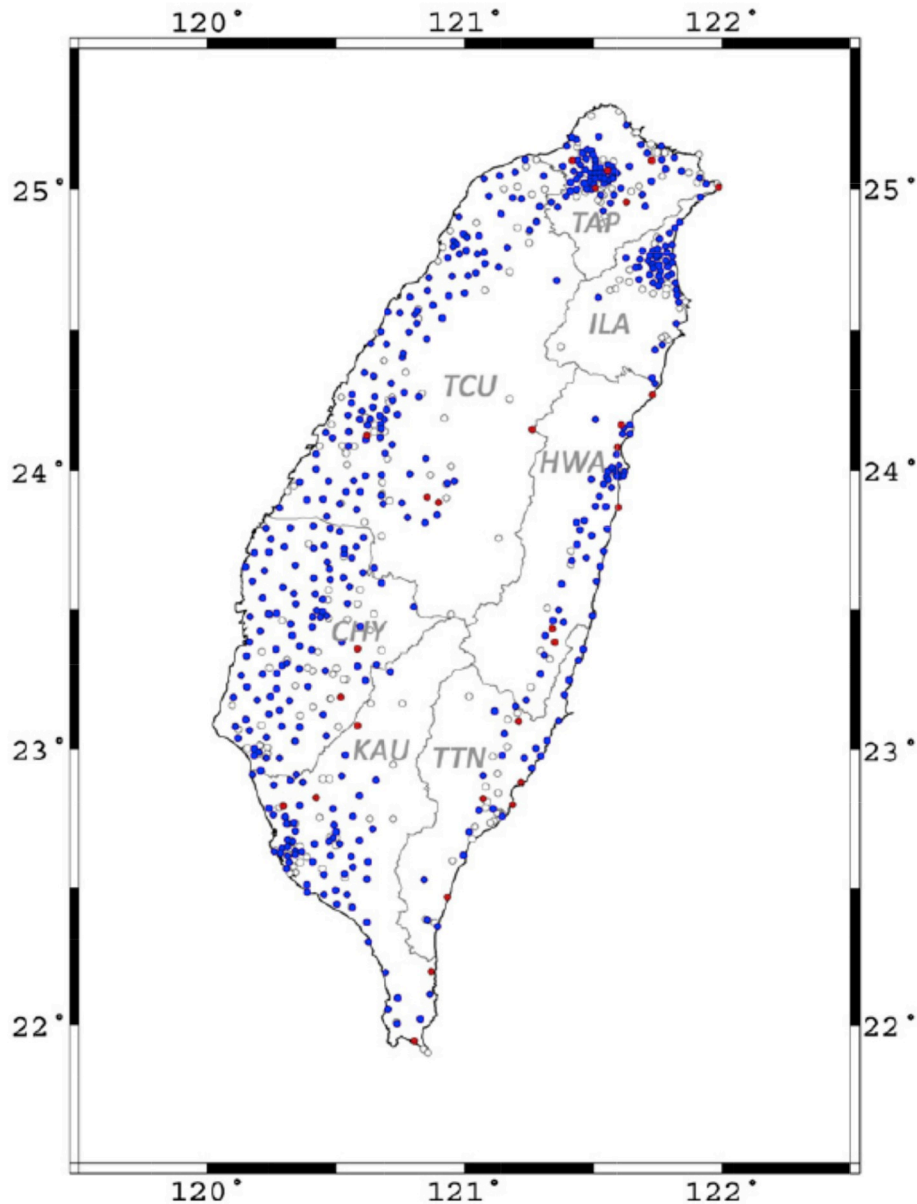


Fig. 1. TSMIP stations.

experimental results. Although Eq. (2) is typically used for estimating small-strain G_o , its form is also applicable for estimating shear modulus G at different strain levels.

A summary by Ref. [14] indicates that n is mostly 0.5 for sand and various types of clays at small strain level (i.e., $n = 0.25$ for V_s according to Eq. (1)) based on 11 proposed models. Kishida and Tsai [12] reported that no clear dependency of n on soil type exists based on the analysis of field data and many previous studies, but the exponent n is site-specific variable depending of several factors such as geologic age and depositional environment. Ku, et al. [15] similarly concluded that the variation of n is site-specific base on the in-situ V_s measurements. Therefore, the soil type is not a major factor that reflects the influence of confining stress on V_s . However, n in Eq. (2) increases according to laboratory test data [13] from $1/3$ – $1/2$ to 1.0 as shear strain γ increases from $10^{-4}\%$ to $10^{-2}\%$ (i.e., the exponent term of σ'_0 changes from $1/6$ – $1/4$ to 0.5 for V_s). The change in n indicates that confining stress influences small- and large-strain soil properties differently. Therefore, the exponent n is strain-dependent, which implies that small-strain property (e.g., V_s or G_o) and large-strain measurement (e.g., N) must be modeled by confining stress differently. Consequently, confining stress

should be included when establishing the correlation between N and V_s . Brandenburg et al. [10] also suggested the inclusion of confining stress to derive the V_s – N correlation.

2.2. Other Factors that Influence Functional Form

Hardin [16] discussed the model form of G_o for normally consolidated (NC) and overly consolidated (OC) clays and suggested the following:

$$G_o = A \cdot F(e) \text{OCR}^k (\sigma'_0)^n, \quad (3)$$

where k can be approximated as

$$k \approx \frac{PI}{160}. \quad (4)$$

The equation implies the following. First, for a non-plastic or low PI soil (e.g., sand or silt), G_o is independent of OCR. Second, given $\text{OCR} = 1$ (NC clay), Eq. (3) yields Eq. (2) and exponent n is a constant regardless of PI. Third, the impact of confining stress on G_o is uncoupled with OCR. Viggiani and Atkinson [17] also reported that the impact of

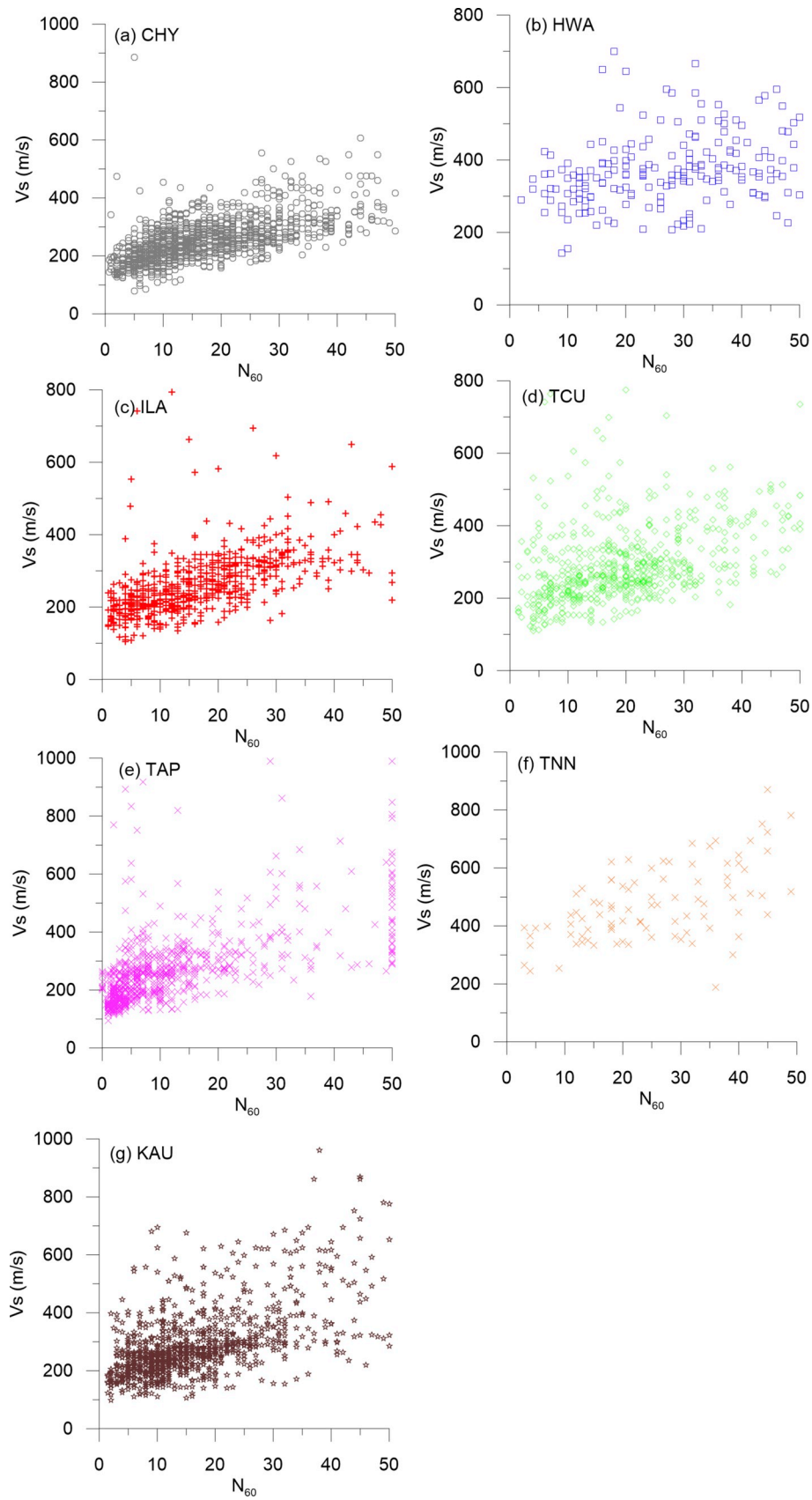


Fig. 2. V_s versus N in different regions.

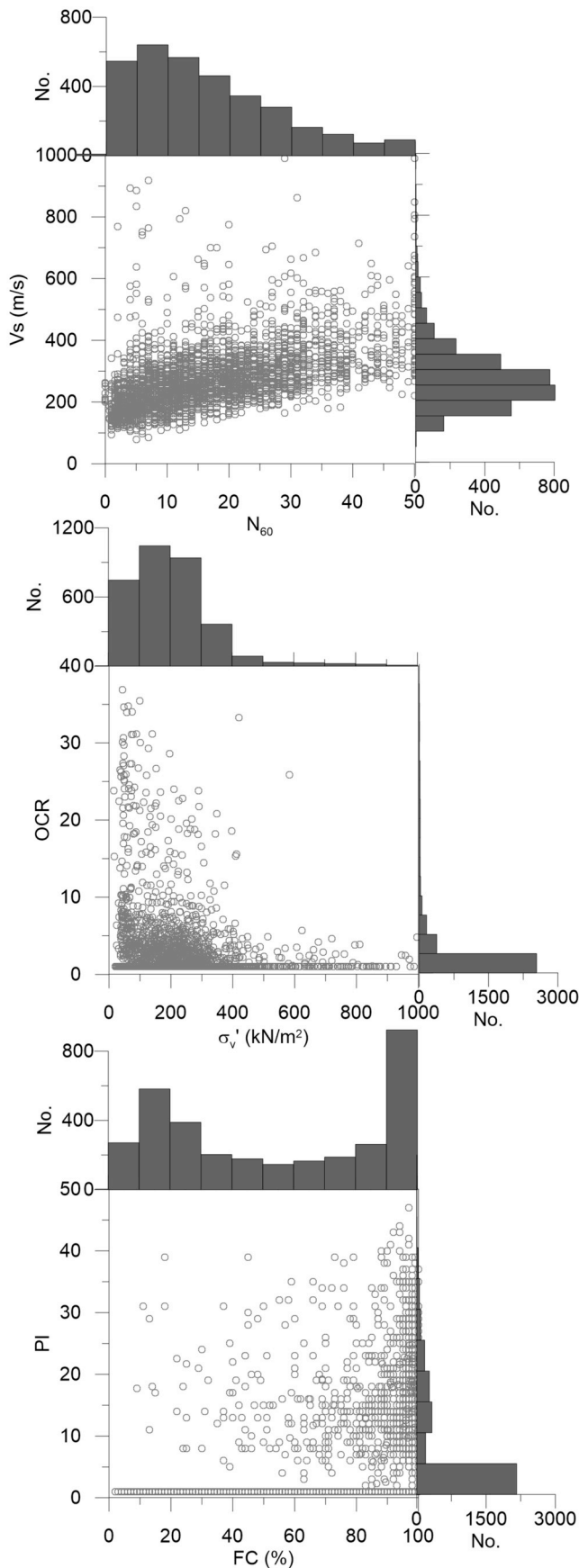


Fig. 3. Distribution of datasets.

confining stress on G_o is uncoupled with OCR as

$$G_o = B(\sigma'_o)^n OCR^m. \quad (5)$$

However, B , n , and m are dependent on PI as revealed by laboratory test results. Kawaguchi and Tanaka [18] proposed a semi-theoretical form of G_o based on the field data as follows:

$$G_o = 20000 \cdot w_L^{-0.8} \cdot \left(\frac{2}{3} OCR\right)^{0.2} \cdot \left(\frac{1 + OCR^{0.5}}{3}\right)^{0.6} \cdot (\sigma'_v)^{0.8}, \quad (6)$$

where σ'_v is effective vertical stress, w_L is the liquid limit, which is similar to the role of PI in Eq. (3). Unlike Eqs. (2), (3) and (5) that are derived using σ'_o from the laboratory data, σ'_v is used in Eq. (6) because σ'_v is easily obtained from the field data. Eq. (6) indicates that the effect of OCR and PI (or w_L) on G_o is uncoupled unlike that in Eq. (3), where the influence of OCR and PI on G_o is coupled.

In addition to the OCR and PI, several studies found that FC can influence the measurement of G_o [19–22]. Based on the laboratory test of specimen with non-plastic fines up to 25%, Wichtmann et al. [19] found that higher FCs result in low G_o and proposed a correct factor f_r (FC) to G_o with FC other than zero. Ruan et al. [22] Performed bender element test on saturated sand-fines mixtures with FC up to 100%. For the mixtures in loose (Relative density, $Dr = 35\%$) or medium dense ($Dr = 50\%$) condition, the G_o decreases sharply and then increases slightly with the increase of FC. However, the G_o only decreases with the increase of FC when the mixture is in dense ($Dr = 60\%$) condition.

2.2. Proposed model form

Based on the review of previous studies, the small-strain properties are dependent on e , σ'_o (or σ'_v), PI, OCR, and FC. σ'_v is considered instead of σ'_o as the model variable because it can be simply estimated from the field data. By contrast, obtaining reliable in-situ void ratio is difficult, especially for sands from the field borings. Thus, void ratio is not considered in the model. The influence of these parameters can be coupled or decoupled. Therefore, two possible regression models of G_o are proposed as follows:

$$\text{Model 1: } \ln(V_s) = a_0 + a_1 \ln(\sigma'_v) + a_2 \ln(FC) + a_3 \ln(PI) + a_4 \ln(OCR), \quad (7)$$

$$\text{Model 2: } \ln(V_s) = a_0 + a_1 \ln(\sigma'_v) + a_2 \ln(FC) + a_3 PI \ln(OCR). \quad (8)$$

The effect of PI and OCR on G_o is uncoupled in Model 1 and coupled in Model 2. Determining which model is superior remains unknown because the coupling effect between PI and OCR is still under debate as discussed earlier. An improved model based on the regression analysis results will be suggested later. Analogically, the general model for N is proposed as follows:

$$\text{Model 1: } \ln(N) = b_0 + b_1 \ln(\sigma'_v) + b_2 \ln(FC) + b_3 \ln(PI) + b_4 \ln(OCR), \quad (9)$$

or

$$\text{Model 2: } \ln(N) = b_0 + b_1 \ln(\sigma'_v) + b_2 \ln(FC) + b_3 PI \ln(OCR) \quad (10)$$

SPT-N generally ranges with effective overburden stresses depending on soil types such as clay, silt, and sand (e.g. Ref. [10]). However, other factors such as stress histories, soil layering, and geologic age also influence on the variation of SPT-N; therefore, the variation of SPT-N with overburden stress is considered as site-specific as similar to the variation of n for V_s [12]. The correction of N due to FC as indicated in the preceding Eq. is usually accounted for when estimating liquefaction resistance based on N [23–25]. As discussed earlier, confining stress influences small- and large-strain soil properties differently. Similarly, the influence of FC and PI on small- and large-strain properties can be potentially different. DeJong et al. [26] found that cementation (one factor causing $OCR > 1$ per Terzaghi et al. [27]) changes the small- and large-strain properties differently. V_s of cemented specimens increased by a factor of 4 but converged with the uncemented specimen at large strains under triaxial test. Therefore, the different effects of these variables on V_s and N will be explored later.

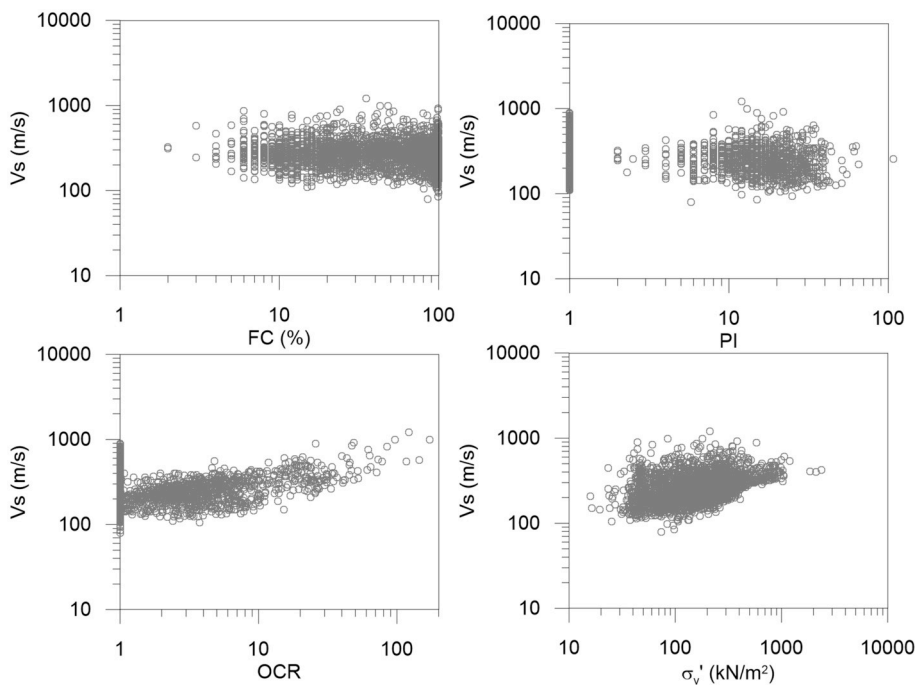


Fig. 4. V_s against model parameters in log–log space.

Table 1
Regression analysis results of Model 1.

	Intercept	Exponent				R^2	σ_{in}	ρ_{NVs}
		σ'_v (kPa)	FC (%)	PI (-)	OCR (-)			
N (-)	0.90	0.58	-0.27	-0.37	0.40	0.50	0.61	0.32
V_s (m/s)	4.59	0.26	-0.08	-0.18	0.32	0.42	0.28	
Ratio	-	2.25	3.43	2.05	1.26	-	-	-

Table 2
Regression analysis results of Model 2.

	Intercept	Exponent				R^2	σ_{in}	ρ_{NVs}
		σ'_v (kPa)	FC (%)	PI (-)	OCR (-)			
N (-)	1.1	0.55	-0.37	-0.00011	-	0.39	0.68	0.45
V_s (m/s)	4.63	0.25	-0.11	0.0042	-	0.33	0.38	
Ratio	-	2.16	3.44	-0.027	-	-	-	-

3. Conditional prediction approach

Multivariable regression is typically adapted for correlating V_s and N and other influence factors (e.g. Refs. [9,10]). However, due to the potential of high correlation between two predictor variables (e.g., N and σ'_v), which is called multicollinearity, multivariable regression may be unsuitable for correlating V_s and N [12]. Therefore, the conditional prediction approach proposed by Kishida and Tsai [12] is adopted instead of multivariable regression in this study. In the Kishida and Tsai approach [12], the model of N and V_s (e.g., Eqs. (7) - (10)) are first determined through separate regression analyses. Then, the relationship between V_s and N (V_s conditional on N) is established based on the correlation of the residual in the model of N and V_s . As a simple example, the following two regression models that only include the confining stress term are used to illustrate the conditional prediction approach.

$$\ln N = b_0 + b_1 \ln \sigma'_v + \varepsilon_N, \tag{11}$$

$$\ln V_s = c_0 + c_1 \ln \sigma'_v + \varepsilon_{Vs}, \tag{12}$$

where ε_N and ε_{Vs} are the residuals and follow the normal distributions with mean = 0 and standard deviation of σ_{lnN} and σ_{lnVs} , respectively. The correlation between ε_N and ε_{Vs} is ρ_{NVs} . Therefore, the conditional prediction of $\ln V_s$ given $\ln N$ is theoretically expressed as follows:

$$E[\ln V_s | \ln N] = \beta_0 + \beta_1 \ln N + \beta_2 \ln \sigma'_v, \tag{13a}$$

where

$$\beta_0 = c_0 - b_0 \frac{\sigma_{lnVs}}{\sigma_{lnN}} \rho_{NVs}, \tag{13b}$$

$$\beta_1 = \frac{\sigma_{lnVs}}{\sigma_{lnN}} \rho_{NVs}, \tag{13c}$$

$$\beta_2 = c_1 - b_1 \frac{\sigma_{lnVs}}{\sigma_{lnN}} \rho_{NVs}, \tag{13d}$$

and

$$\sigma_{Vs|N}^2 = \sigma_{Vs}^2 (1 - \rho_{NVs}^2). \tag{14}$$

Based on the preceding procedure, the correlation between V_s and N can be established through the individual correlation of V_s (or N) with the model parameters. The conditional approach can be extended in a similar manner when additional terms (e.g., FC, PI, and OCR in Eqs. (7) and (9)) are added to Eqs. (11) and (12)).

4. Database for regression analysis

The data provided in EGDT include stratum description, results of soil physical property tests (such as grain size distribution, uniformity coefficient, coefficient of gradation, void ratio, water content, specific gravity, unit weight, liquid limit, and PI), soil classification, P- and S-wave velocities, and SPT-N values. EGDT provides sufficient information for the regression analysis in addition to the measurement of N and V_s . However, the required model parameter OCR is unavailable in EGDT. Therefore, OCR is approximately estimated by Eq. (6) in this study given the measured V_s (or G_o), w_L and σ'_v in the database. The

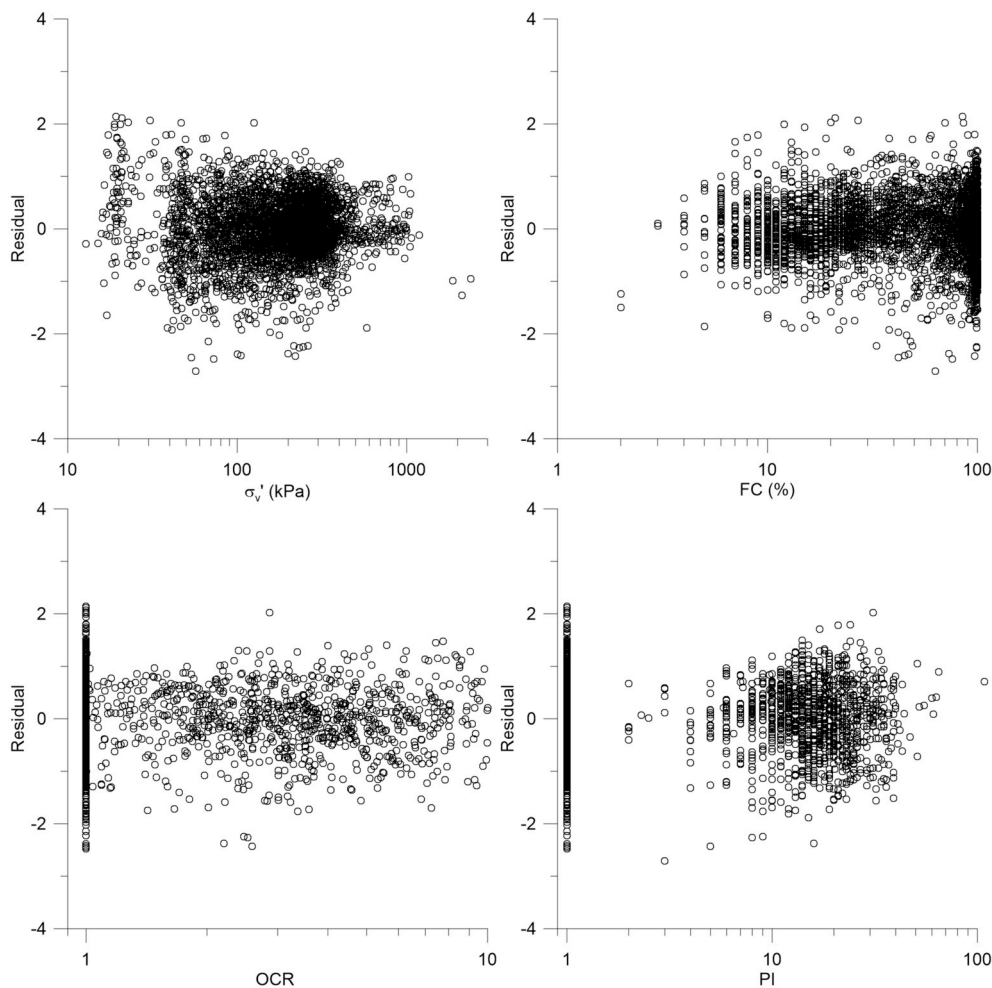


Fig. 5. Residual of N prediction based on Eq. (9).

influence of this assumption will be explored later in the paper. Effective overburden stresses σ_v' are calculated with the given depth, unit weight, and water table elevation. Groundwater elevation is occasionally not recorded for some borings. In such cases, the P-wave velocity profile is utilized to identify the approximate elevation of the groundwater table. An abrupt transition from P-wave velocity lower than 500 m/s to higher than 1500 m/s is typically apparent in boring logs, clearly indicating the position of the groundwater table.

In EGDT, SPT-N is measured by an automatic hammer falling system every 1.5 m (every 3 m to 5 m for gravel layers) or at the depth of notable discontinuity during drilling. No energy ratio was measured during the drilling. According to Ref. [28], based on 395 pieces of data of 24 borings conducted in Taiwan, the energy ratio varied along the depth in which low energy ratio was observed near the surface and high at depth. The energy ratio is approximately 64% on average. Therefore, the N is corrected to N_{60} by assuming the measured energy ratio of 64%. P- and S-wave velocities are measured with a suspension PS logger system. Velocity measurement is generally performed every 0.5 m, except for several drillings in the first and second years, in which velocity is measured every 1 m.

The boring ID is similar to the codes of the TSMIP stations that were assigned according to the abbreviations of the different regions of Taiwan Island, which are TAP, TCU, CHY, KAU, TTN, HWA, and ILA, as shown in Fig. 1. Notably, these regions are not categorized by its geological unit but simply based on the province. In addition, V_s - N distributions vary in different regions as shown in Fig. 2. The data from TAP, TCU, CHY, HWA, and ILA are used for regression analysis, and the

remaining data (KAU and TTN in the southern region of Taiwan) are employed to verify the model. SPT blow counts that exceed approximately 50 correspond to a refusal condition. Therefore, we excluded the data of N larger than 50 in the database. Furthermore, for non-plastic soil, PI is set as a unity; for soil without FC, FC is also set as a unity. A total of 3,684 data sets from 334 sites that include V_s , N , σ_v' , FC, PI, and estimated OCR are used for the regression analysis. As shown in Fig. 2, there are some data points with very high V_s but very low N due to inherent errors in the database. Because it is difficult to eliminate these data based on the judgement, all points are used in the regression analysis. Since these erroneous data are few, its influence on the regression results is minor. The distribution of data is shown in Fig. 3. The V_s mostly distribute between 150–400 m/s with mean of 258 m/s; the N mostly distributes between 1–30 with mean of 12.6; the σ_v' is mostly less than 300 kPa with mean of 167 kPa; the OCR is mostly less than 3 with mean of 1.6; the PI is mostly less than 5 with mean of 2.6; the FC evenly distributes between 0% and 100% with mean of 40.7%. The estimated OCR is high near the ground surface and decreases with the depth, which is consistent with the typical trend of field observation [27]. The evenly distributed FC indicates uniformly distributed soil type in the database, which is excellent for developing a unified model. The database consists of clay (29%), silt (21%), sand (47%), and gravel (3%).

Fig. 4 shows the V_s against the model parameters. V_s is approximately linear against the model parameters in log-log space, which indicates that modeling V_s by Eqs. (7)–(8) is sufficient prior to the performance of regression analysis.

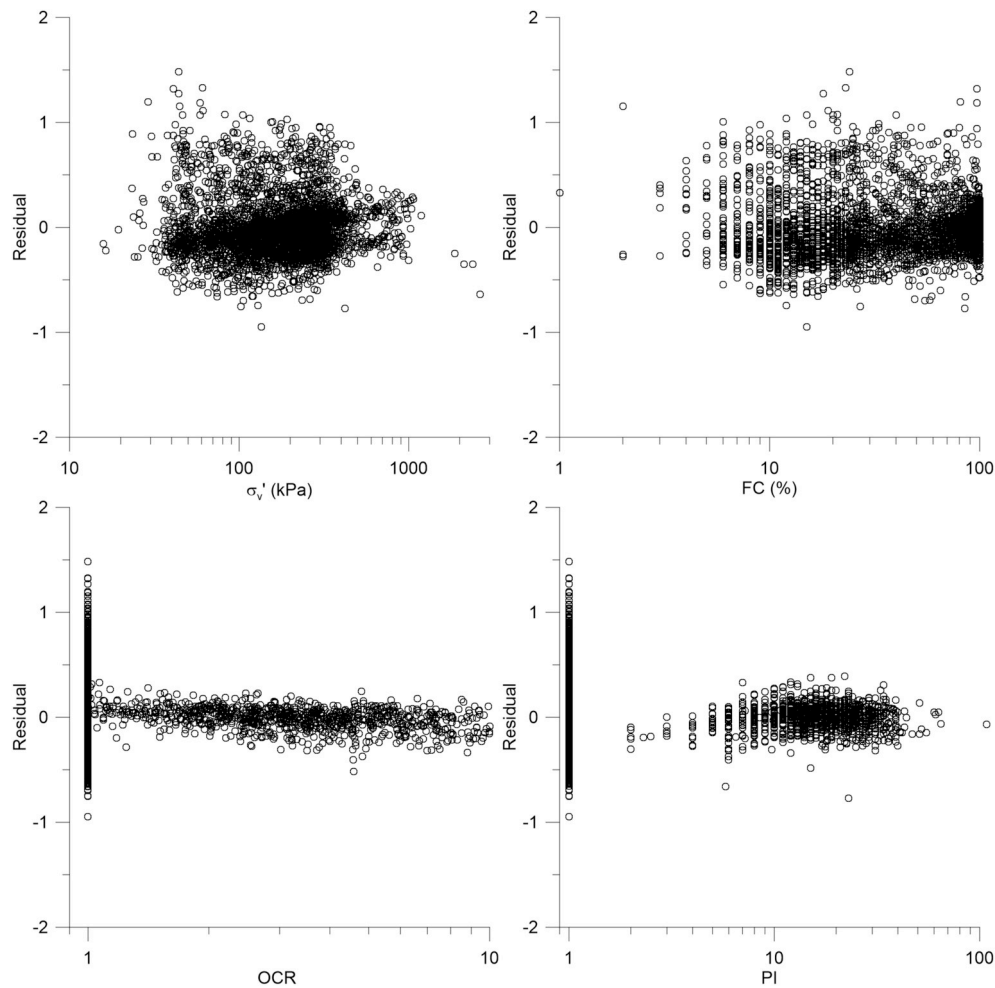


Fig. 6. Residual of V_s prediction based on Eq. (7).

5. Regression analysis results

5.1. Overall results

Table 1 and Table 2 summarize the regression result of Models 1 and 2, respectively. The efficiency of the models is usually evaluated based on the obtained correlation relationship (R^2) and standard deviation (σ_{in}) in the regression analysis. A model with high R^2 and low σ_{in} equates to superior performance. Based on this finding, Model 2 is not as satisfactory as Model 1 because a high σ_{in} is obtained. In addition, the model coefficients for N and V_s in Model 2 are inconsistent. Specifically, the coefficient of PI term is positive for V_s but negative for N . The negative coefficient indicates a high OCR result in low N , which is different from that of stiff clay, which typically has a high blow count. The inconsistent results indicate the possible unsuitability of Model 2. Therefore, Model 1 is adopted and discussed hereafter.

Fig. 5 and Fig. 6 show the residuals of N and V_s of Model 1, respectively. Overall, the models do not demonstrate the bias to all the model variables, indicating the adequacy of the model form. The only bias is exhibited at the confining stress (or the shallow depth) where the mean residual is positive (i.e., underestimated). This bias is the inherent limit of the model that describes the V_s or N as a constant exponential of σ_v' . The predicted V_s or N rapidly decreases and reaches zero as they approach the ground surface, while the measured V_s or N still presents certain values. By contrast, the residual of N exhibits a larger scatter than that of V_s , and even the mean of N is much smaller than that of V_s (i.e. coefficient of variance of N is higher than that of V_s). This observation is consistent with the generally known idea that N

measurement involves additional uncertainty (e.g., method, labor, and energy ratio), thus potentially exhibiting a high variation.

5.2. Difference of small- and large-strain behavior

The difference of physical and mechanical responses of V_s and N can be observed by comparing the regression analysis results of Eqs. (7) and (9). The V_s is connected with small-strain responses whereas the N is more associated with large-strain ones. Table 1 shows that the exponent terms of σ_v' and OCR are positive, whereas those of FC and PI are negative for N and V_s , respectively. Therefore, these variables exhibit similar influence on small-strain properties and large-strain measurements. The positive values indicate that N and V_s increase with OCR and σ_v' , and the negative values indicate that both properties decrease as FC and PI increase. These trends are consistent with the previous study of G_o observed from the lab tests [14,16,18,19]. However, the value of the exponent term is different for N and V_s . The exponent term of σ_v' for V_s (small-strain property) is approximately 0.25, whereas that for N (large-strain measurement) is approximately 0.5, which are both consistent with the values suggested by Refs. [14,29] for V_s and N , respectively.

Different values of predictor variables represent varying degrees of influence on N and V_s . High absolute value indicates a considerable influence on N or V_s . Therefore, the relative influence of these variables on large- and small-strain behavior can be quantified by the ratio of coefficients between N and V_s , in which the highest value implies the largest effect on N relative to the effect on V_s . Based on this understanding, the influence of FC is largest on N relative to V_s , followed by

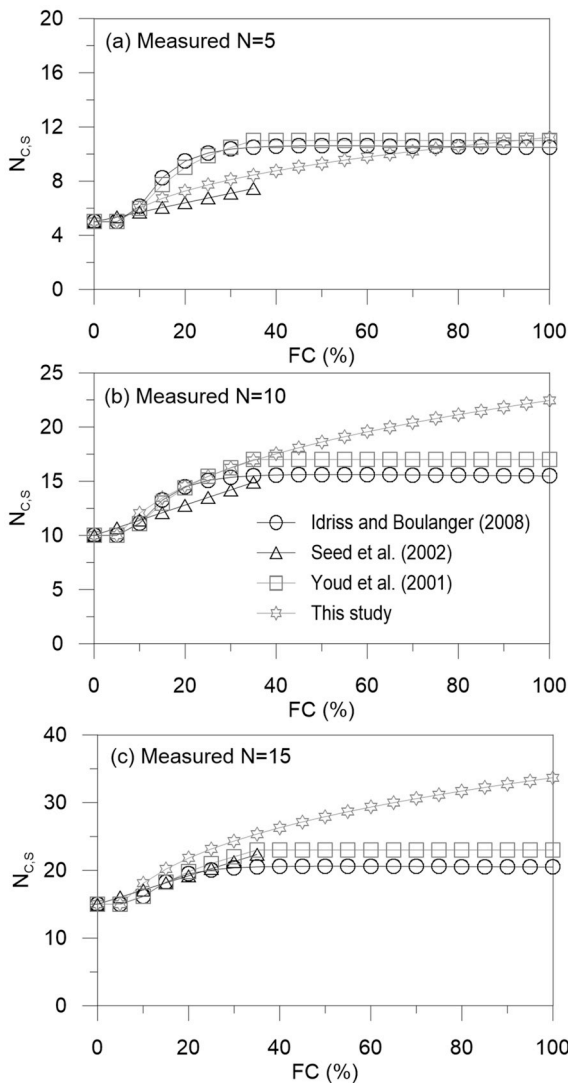


Fig. 7. Comparison of corrected N for various FCs with given measurements of N = 5, 10, and 15.

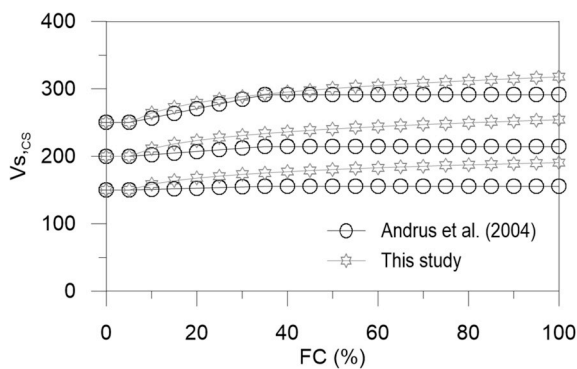


Fig. 8. Comparison of corrected V_s for various FCs with given measurements of V_s (at FC = 0%) = 150, 200, and 250 m/s.

σ_v' , PI, and OCR as shown in Table 1. Such difference should be considered when developing the correlation between N and V_s . With σ_v' as an example, the obtained exponent ratio is approximately 2, which is similar to that reported by Ref. [10]. Therefore, if V_s is correlated to N, then the influence of σ_v' is not negligible. In other words, the prediction model of V_s based on N should also include the σ_v' term, as suggested by

Ref. [10]. Similarly, FC and PI should also be included in the model mainly due to their different influences on small- and large-strain behavior, respectively. Only the ratio of OCR is approximately 1. Thus, the prediction model of V_s based on N can possibly exclude the OCR term if the product of $\frac{\sigma_v'}{\sigma_N}$ and ρ_{NV_s} is approximately 1 according to Eq. (14d).

5.3. Influence of FC

The developed correlation between N and FC and V_s and FC can also be utilized to evaluate the influence of FC on V_s and N. The coefficient of FC for N is higher than that for V_s , indicating that FC has more influence on N than V_s . In the liquefaction potential analysis, N and V_s require further correction to estimate the liquefaction resistance of soil containing certain amounts of fines. Corrected (or equivalent) N or V_s is typically higher than the measured N or V_s for soil with certain FC. The negative coefficient of FC obtained in this study is consistent with the concept of correction for FC in the liquefaction analysis. We also quantitatively compared FC correction from our regression analysis with that proposed by previous studies. Fig. 7(a) shows a comparison of FC-corrected N (N_{cs}) by Refs. [23,24], and [25] for various FCs with given measurements of N = 5, 10, 15. N_{cs} in this study is calculated as follows:

$$N_{cs} = N / FC^{-0.27}. \tag{15}$$

The above equation is derived based on Model 1 (Eq. (9)) and the obtained regression coefficient b2 in Table 1. Notably, Eq. (15) is only applicable to the condition of N < 15 for all FCs or all N for FC < 30% based on the database distribution. Given measurements of N = 5 and 10, the N_{cs} in this study is in the range of the N_{cs} obtained by the other studies. For N = 15, the N_{cs} in this study is slightly larger than that suggested by others. The previous studies mostly consider N correction with FC up to 35%. By contrast, the result of this study indicates that N may be further influenced by a high FC. Such influence is considered mechanical correction during the SPT measurement and may not be necessary for the correction of liquefaction resistance.

We also compared FC-corrected V_s ($V_{s,cs}$) in this study with that corrected by Ref. [30] for various FCs and three given measurements of V_s . $V_{s,cs}$ in this study is calculated as follows:

$$V_{s,cs} = V_s / FC^{-0.08}. \tag{16}$$

The above equation was derived based on Model 1 (Eq. (7)) and the obtained regression coefficient a2 in Table 1. As shown in Fig. 8, the $V_{s,cs}$ in this study is slightly higher than that in Ref. [30] for low measured V_s but agrees well with that in Ref. [30] for measured $V_s = 250$ m/s. Similar to the influence of FC on N, V_s may be further corrected for a higher FC, as indicated by our regression model compared to Ref. [30] that is only applied for FC < 35% in. The decreasing trend of V_s with FC > 35% is consistent with the behavior of the dense sand-fines mixtures reported by Ref. [22] but different from that of the loose to medium mixtures. Void ratio or relative density also influences the dependency of V_s on FC. Since the proposed model is based on the field data that covers a wide range of soils with different void ratios, relative densities, and properties of fines, the obtained result may represent an "apparent" behavior compared to that in the laboratory for a specified condition (i.e. non-plastic fines and a constant void ratio or relative density). The correction of V_s due to high FC for different conditions needs to be further clarified by the laboratory test.

5.4. Unified vs prediction model

A unified empirical model is developed according to the previously described conditional prediction procedure (Eqs. (11) to (14)). Given the regression result of Eqs. (7) and (9) as listed in Table 1, the proposed model is,

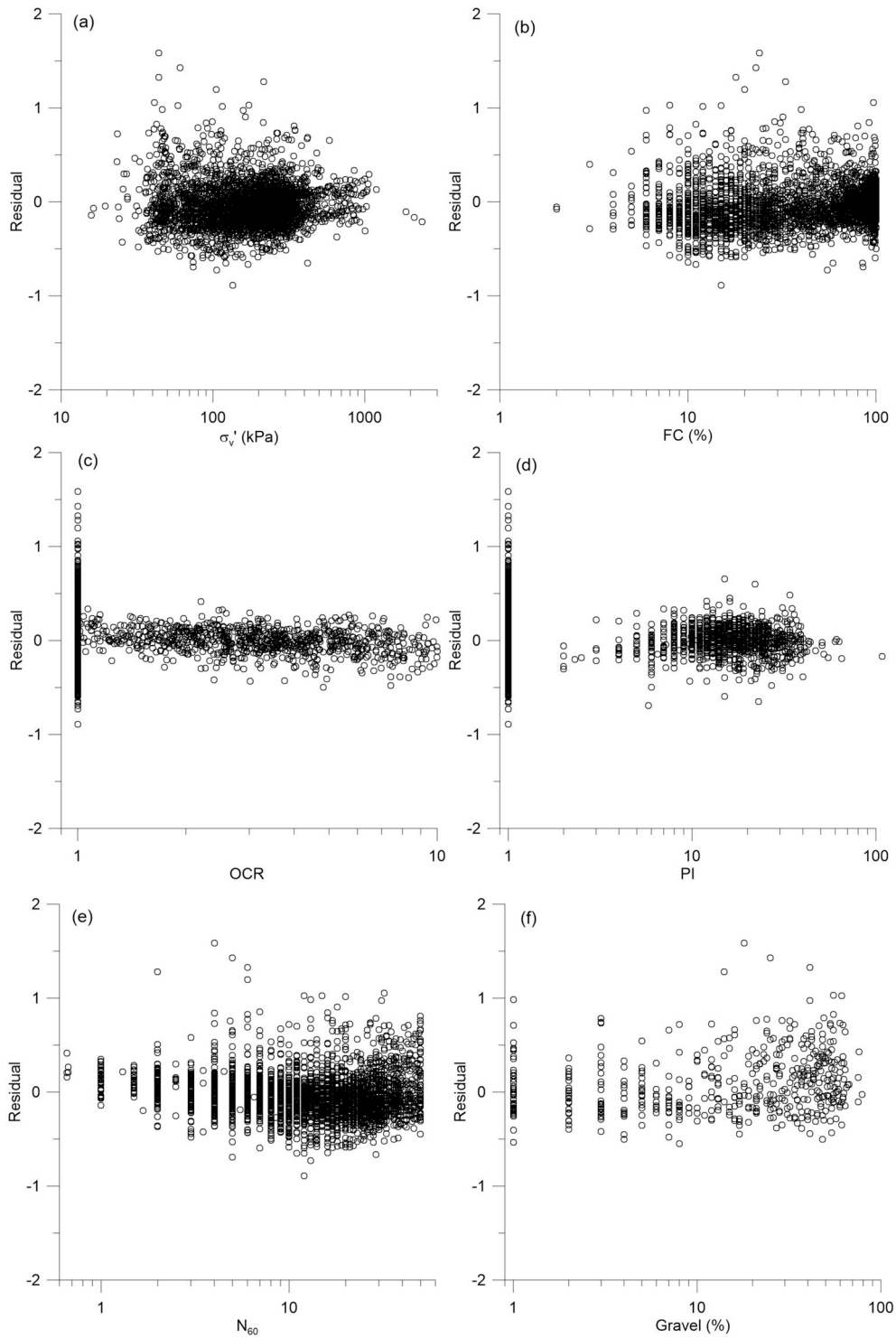


Fig. 9. Residual of V_s prediction based on Eq. (17).

$$\ln V_s = 4.46 + 0.15 \ln N_{60} + 0.17 \ln \sigma'_v - 0.04 \ln FC - 0.12 \ln PI + 0.26 \ln OCR \quad (17)$$

R^2 is 0.45 and the standard deviation of σ_{\ln} is 0.26, which is approximated as $\sigma = 63$ m/s given mean $V_s = 270$ m/s. The residual of V_s prediction condition on N is shown in Fig. 9. Overall, the models do not show a clear bias to the model variables, indicating the adequacy of the model form. Moreover, the biases shown at the low confining stress in Figs. 5 and 6 are not observed in Fig. 9. This finding can be attributed to the conditioning of V_s on N , in which the preceding bias mentioned is

automatically corrected through Eq. (13d) by including the correction of residual of Eqs. (7) and (9). Fig. 9(f) also presents the residual against the gravel content in addition to that of FC in Fig. 9(d). The absence of bias to gravel content and FC indicates that the model can be applied for a wide range of soil types, including gravel, sand, silt, and clay. However, given that the database only has 3% of gravel, the applicability of the model requires further evaluation.

In Ref. [11], the dataset similar to that used in the present study was grouped into clay and sand for regression analysis, and the obtained σ of the individual V_s - N model were 67 m/s and 77 m/s. Although we

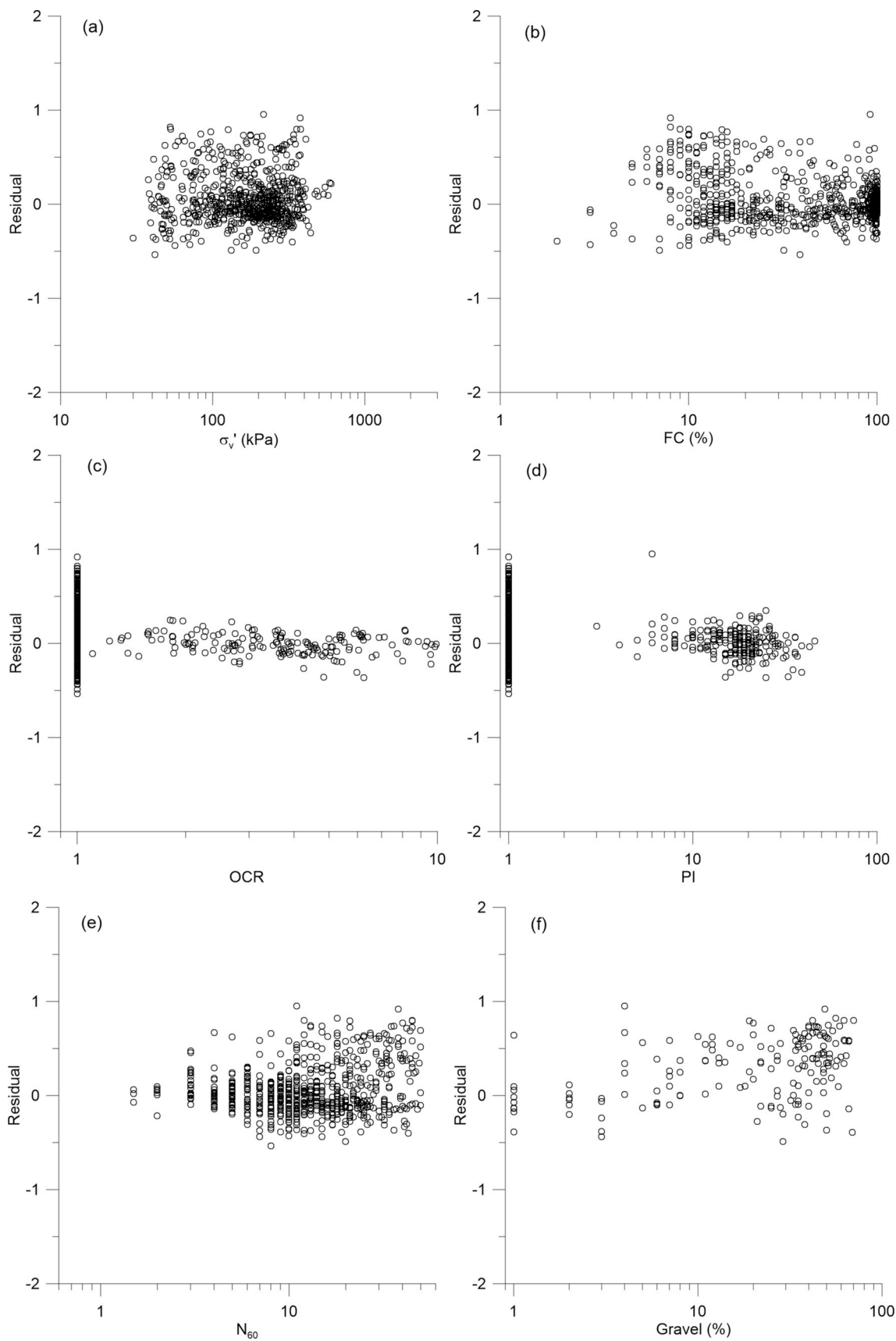


Fig. 10. Residual of V_s prediction using KAU and TTN data.

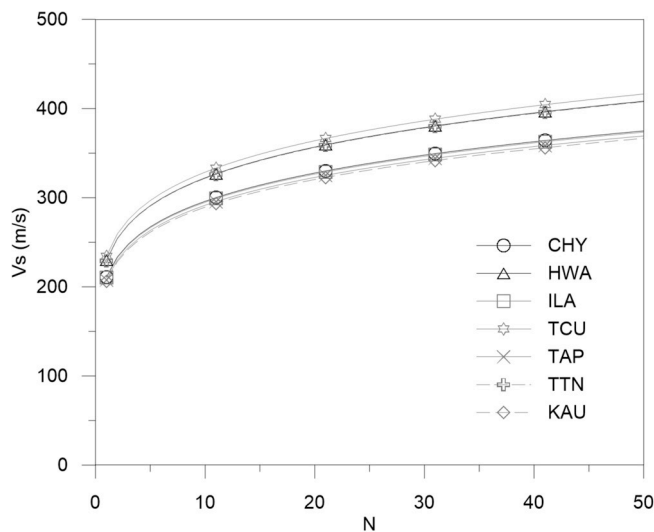


Fig. 11. V_s prediction of different regions given $\sigma_v' = 300$ kPa and mean of FC, OCR, and PI.

used the entire dataset in the regression analysis, the standard deviation obtained in the present study is lower than that reported by Ref. [11]. The model that includes additional prediction parameters, such as FC and PI, considerably improve the prediction accuracy. The model can be applied to general conditions for estimating V_s by N and is not limited to a specific soil type.

Considering that OCR is not directly provided in the database and indirectly estimated, we also evaluate the model performance if OCR is excluded from the model. The result shows that removing OCR from the model has a limited effect because σ is slightly increased from 63 m/s to 68 m/s given mean $V_s = 270$ m/s. The model based on σ_v' , FC, and PI can sufficiently predict V_s , and even OCR is typically unavailable in practice. This result may be mainly due to the similarity of the OCR influence on small- and large-strain properties as discussed earlier. Therefore, the following equation can be adopted if OCR is unavailable:

$$\ln V_s = 4.52 + 0.22 \ln N_{60} + 0.11 \ln \sigma_v' - 0.03 \ln FC + 0.02 \ln PI \quad (18)$$

R^2 is 0.35 and σ_{in} is 0.29. If the model form only includes σ_v' as typically modeled by others (e.g. Ref. [10]), then σ becomes high ($V_s = 94$ m/s). Nevertheless, σ is still lower than the value of approximately 103 m/s obtained by Ref. [11] for the entire dataset. This improvement may be attributed to the conditional prediction approach adopted in this study and the use of σ_v' instead of depth in the model.

6. Verification

The data of KAU and TTN (683 datasets) in the southern region of Taiwan are used to verify the proposed model. The standard deviation of the prediction σ_{in} is 0.26, which is similar to that obtained by regression analysis. However, the mean residual is 0.058, which is slightly larger than zero. The small positive value indicates a slight underestimation of V_s (approximately 10 m/s given mean $V_s = 270$ m/s) but is acceptable compared with the magnitude of σ_{in} . Fig. 10 shows the residual against different variables. Once more, the models do not reveal the clear bias to the model variables.

Kuo et al. [11] proposed 12 different models to predict V_s for different soil types and regions. By contrast, this study only used one unified model to successfully predict all soil types in different regions. In addition, the prediction accuracy is further improved in terms of low σ_{in} . Fig. 11 shows the V_s prediction for different regions given $\sigma_v' = 300$ kPa and mean of FC, OCR, and PI by the regions. Similar to the results reported by Ref. [11], TCU, TTN, and HWA exhibit higher V_s than other regions. This condition can be attributed to low FC or high

gravel content as measured in these regions. However, the proposed correlations do not include gravel contents as a parameter. In addition, the analyzed dataset excluded the data with $N > 50$. Therefore, this study cannot measure the influence of gravel contents on the resulted correlations. Overall, the proposed unified model effectively captures the variation of V_s in the different regions by accounting for the regional feature of soil properties.

7. Conclusions

Numerous relations between N and V_s have been proposed for practical purposes in earthquake engineering. However, these empirical correlations significantly vary in terms of model form and parameters. Without a theoretical or experimental basis, these correlations are only developed by statistical method and for a specific site and soil type. V_s and N are typically considered small- and large-strain properties, respectively. Such difference should be considered in the development of the model to correlate N and V_s . Therefore, a unified empirical correlation model was established in this study using a conditional prediction approach to correlate small- and large-strain properties based on EGDT with 3684 datasets.

The main factors that can change the small-strain property include σ_v' (or σ_v'), FC, PI, and OCR according to a previous study on laboratory test data. Therefore, we developed a simple model form that includes these parameters to estimate small-strain property and applied it to large-strain measurement similarly. The influence of these parameters on small-strain properties (i.e., V_s) and large-strain measurements (i.e., N) was discussed according to the regression result. Different exponent values of predictor variables stand for varying degrees of influence by these parameters on large- and small-strain properties. As indicated by the ratio of coefficients between N and V_s , FC influences N and V_s most differently, followed by σ_v' , PI, and OCR. The coefficient ratio for σ_v' between N and V_s is approximately 2, which is consistent with that in previous studies. In addition, the influence on N and V_s by FC based on the regression result agrees well with the fine correction recommended in the liquefaction potential analysis.

Last, a unified correlation model between V_s and N that is dependent on σ_v' , FC, PI, and OCR was established through a conditional prediction approach. The model, which included additional prediction parameters, such as FC, OCR, and PI, successfully predicted the V_s of a wide range of soil types in the different regions of Taiwan and exhibited a high variation of V_s . The proposed model can be applied to general conditions (i.e. the other regions in Taiwan) and is not limited to a specific soil type. However, the user should employ the model for gravel with caution due to the relatively small amount of data utilized in model development.

Acknowledgments

We would like to express our special thanks to H.Y. Hsu and C. L. Wen for managing the database. This work was supported by the Ministry of Science and Technology, Taiwan, under Award No. MOST 105-2628-E-005-002-MY3. The authors gratefully acknowledge such support.

Appendix A. Supplementary data

Supplementary data to this article can be found online at <https://doi.org/10.1016/j.soildyn.2019.105783>.

References

- [1] Kramer SL. Geotechnical earthquake engineering. Upper Saddle River, N.J.: Prentice Hall; 1996.
- [2] Power M, Chiou B, Abrahamson N, Bozorgnia Y, Shantz T, Roblee C. An overview of the NGA project. Earthq Spectra 2008;24:3–21.

- [3] Stewart JP, Seyhan E. Semi-empirical nonlinear site amplification and its application in NEHRP site factors. PACIFIC EARTHQUAKE ENGINEERING RESEARCH CENTER. 2013. p. 60.
- [4] Dikmen U. Statistical correlations of shear wave velocity and penetration resistance for soils. *J Geophys Eng* 2009;6:61–72.
- [5] Pitilakis K, Raptakis D, Lontzetidis K, Tika-Vassilikou T, Jongmans D. Geotechnical and geophysical description of Euro-Seistests, using field, and laboratory tests and moderate strong ground motions. *J Earthq Eng* 1999;3:381–409.
- [6] Sykora DE, Stokoe KH. Correlations of in-situ measurements in sands of shear wave velocity. *Soil Dyn Earthq Eng* 1983;20:125–36.
- [7] Imai T, Tonouchi k. Correlation of N value with S-wave velocity and shear modulus. Proc., 2nd european symp. on penetration testing, amsterdam. 1982. p. 67–72.
- [8] Ohta Y, Goto N. Empirical shear wave velocity equations in terms of characteristic soil indexes. *Earthq Eng Struct Dyn* 1978;6:167–87.
- [9] Kwak DY, Brandenburg SJ, Mikami A, Stewart JP. Prediction equations for estimating shear-wave velocity from combined geotechnical and geomorphic indexes based on Japanese data set. *Bull Seismol Soc Am* 2015:105.
- [10] Brandenburg SJ, Bellana N, Shantz T. Shear wave velocity as function of standard penetration test resistance and vertical effective stress at California bridge sites. *Soil Dyn Earthq Eng* 2010;30:1026–35.
- [11] Kuo C-H, Wen K-L, Hsieh H-H, Chang T-M, Lin C-M, Chen C-T. Evaluating empirical regression equations for vs and estimating Vs30 in northeastern Taiwan. *Soil Dyn Earthq Eng* 2011;31:431–9.
- [12] Kishida T, Tsai C-C. Prediction model of shear wave velocity by using SPT blow count based on the conditional probability framework. *J. Geotech. Geoenviron. Eng.* 2017;143.
- [13] Ishihara K. Soil behavior in earthquake geotechniques. Oxford: Clrendon Press; 1996.
- [14] Kokusho T. In situ dynamic soil properties and their evaluation. 8th asian regional conference on soil mechanics and foundation engineering, Kyoto, Japan. 1987. p. 215–35.
- [15] Ku T, Subramanian S, Moon SW, Jung JW. Stress dependency of shear wave velocity measurements in soils. *J Geotech Geoenviron Eng* 2017;143.
- [16] Hardin BO, Black WL. Vibration modulus of normally consolidated caly. *J. Soil Mech. Found. Div. Am. Soc. Civ. Eng.* 1968;94:353–69.
- [17] Viggiani G, Atkinson JH. Stiffness of fine-grained soil at very small strains. *Geotechnique* 1996;45:249–65.
- [18] Kawaguchi T, Tanaka H. Formulation of Gmax from reconstituted clayey soil its application to measured Gmax in the field. *Soils Found* 2008;48:821–31.
- [19] Wichtmann T, Navarrete Hernández MA, Triantafyllidis T. On the influence of a non-cohesive fines content on small strain stiffness, modulus degradation and damping of quartz sand. *Soil Dyn Earthq Eng* 2015;69:103–14.
- [20] Kao Y-H. Study of dynamic properties of soil mixtures. Civil engineering. National Taiwan University; 2015.
- [21] Chien KL, Oh YN. Influence of fines content and initial shear stress on dynamic properties of hydraulic reclaimed soil. *Can. Geotech. J.* 2002;39:242–53.
- [22] Ruan B, Miao Y, Cheng K, Yao E. Study on the small strain shear modulus of saturated sand-fines mixtures by bender element test. *Eur. J. Environ. Civ. Eng.* 2018. <https://doi.org/10.1080/19648189.2018.1513870>.
- [23] Idriss IM, Boulanger RW. Soil liquefaction during earthquakes. EERI; 2008.
- [24] Seed RB, Cetin KO, Moss RES, Kammerer AM, Wu J, Pestana JM, Riemer MF, Sancio RB, Bray JD, Kayen RE, Faris A. Recent advances in soil liquefaction engineering: a unified and consistent framework. 26th annual geotechnical spring seminar, los angeles section of the GeoInstitute. Queen Mary, Long Beach, CA: American Society of Civil Engineers; 2003.
- [25] Youd TL, Idriss IM, Andrus RD, Arango I, Castro G, Christian JT, Dobry R, Finn WDL, Harder Jr. LF, Hynes ME, Ishihara K, Koester JP, Liao SSC, Marcuson WF, Martin GR, Mitchell JK, Moriwaki Y, Power MS, Robertson PK, Seed RB, Stokoe KH. Liquefaction resistance of soils: summary report from the 1996 NCEER and 1998 NCEER/NSF Workshops on evaluation of liquefaction resistance of soils. *J Geotech Geoenviron Eng* 2001;127:817–33.
- [26] DeJong JT, Fritzes MB, Nusslein K. Microbially induced cementation to control sand response to undrained shear. *J Geotech Geoenviron Eng* 2006;132:1381–92.
- [27] Terzaghi K, Peck RB, Mesri G. Soil mechanics in engineering practice. third ed. ed. New York: Wiley; 1996.
- [28] Huang F-K. Establishment and application of the SPT evaluation model for the liquefaction probability and associated damages. *J. Chin. Inst. Civ. Hydraul. Eng.* 2008;20:155–74.
- [29] Liao SC, Whitman RV. Overburden correction factors for SPT in sand. *J. Geotech. Eng. ASCE* 1986;112:373–7.
- [30] Andrus RD, Piratheepan P, Ellis BS, Zhang J, Hsein Juang C. Comparing liquefaction evaluation methods using penetration-VS relationships. *Soil Dyn Earthq Eng* 2004;24:713–21.